A Novel Wireless Accelerometer Board for Measuring Low-Frequency and Low-Amplitude Structural Vibration.

Alessandro Sabato, Maria Q. Feng, Yoshio Fukuda, Domenico Luca Carní, *Member IEEE*, and Giancarlo Fortino, *Member IEEE*

***Abstract*—Structural Health Monitoring (SHM) plays an important role in maintaining system integrity of aging structures and machinery parts. Micro Electro-Mechanical System (MEMS) accelerometers, because of their low cost and small dimensions, have emerged as attractive sensing tools for monitoring structural condition based on changes in structural vibration characteristics. For SHM applications, these sensors need to detect low-amplitude and low-frequency vibrations. Those are not always feasible with the conventional low-cost digital sensor boards. In this study, a novel accelerometer board, named Acceleration Evaluator (ALE), is developed to achieve more accurate wireless vibration measurements using the full bandwidth of the installed MEMS accelerometer by a Voltage-to-Frequency (V/F) converter, instead of conventional Analog-to-Digital Converter (ADC). The effectiveness of the prototype is evaluated through laboratory tests, demonstrating its measurement accuracy comparable to that of wire-based Integral Electronics Piezoelectric (IEPE) accelerometers. Furthermore, ALE performance for SHM purposes are validated by carrying out shaking table tests on the real-size model of a stone pinnacle of the Washington D.C. National Cathedral.**

***Index Terms*—Wireless telemetry, acceleration measurement, MEMS sensors, system design, structural health monitoring application.**

I. Introduction

ADVANCES made in Micro Electro-Mechanical System (MEMS) technologies and wireless data transmission have created new methodologies for vibration measurements of civil and mechanic structures. Wireless technology is not entirely new and many applications have already been successfully developed (e.g. habitat monitoring [20], [13], environmental parameters detection [2], [4], healthcare [9], [25] and supply chain management [21]). However, these applications do not require high accuracy measurement and high transmission rate, thus data acquisition is relatively easy to achieve. On the other hand, Structure Health Monitoring (SHM) applications require the capability of handling large amount of data, high fidelity sensing, and high-speed data sampling. For instance, measurement systems need to be sensitive in a wide range of accelerations: from 10^{-2} m·s^{-2} (e.g. ambient vibrations) to 10^{1} m·s^{-2} (e.g. earthquakes) [3], [11]. Also, same sensitivity is required in the measurement of low-frequency vibration (10^{-1} - 10^{1} Hz) [5], [14]. Since late '90s on, several accelerometer board prototypes have been developed [10], [18]. Due to cost limitations, the first prototypes employed low-resolution and high-noise-density MEMS sensors [1]. Therefore, it was not possible to accurately measure micro-vibrations [11], [15]. Hence, more sensitive accelerometers [31], with lower noise floor, were used. Nevertheless, measurement accuracy was not improved enough for SHM application. The measurement accuracy also depends on the resolution of quantization by an Analog-Digital Converter (ADC). The first boards, which have 10-bit [15] or 12-bit [36] ADCs, cannot provide suitable resolution for SHM. Therefore, on the board's next generation 16-bit ADCs were employed [14]. As a result, the limiting factor to measurements precision became the precision of the accelerometer itself. For this reason, the sensor bandwidth and measurement range were reduced to improve board resolution matching it to that of the embedded ADC [12], [14], [24]. This operation narrows the fields of applicability and it limits board usage to other vibrating systems. Furthermore, the system limits the lowest detectable to nearly 1 Hz. Other researches to improve the comprehensive sensing performance based on software technologies have been studied, such as the construction of scalable networks [23], the performances of the network itself [6], [33], and on creating embedded algorithms for reducing transmitted data volume [7], however, the solution for the fundamental problem of the sensing accuracy is not been presented.

In this study, to cope with these problems, the Acceleration Evaluator (ALE) [28], a MEMS accelerometer board, is used to achieve accurate wireless vibration measurement, even if the vibration has low amplitude and frequency. The wireless transmission capability resolves following problems: (i) wire impedance (i.e. necessity to install amplifiers), (ii) noise produced (i.e. triboelectric noise), and (iii) mounting facility.

ALE effectiveness for SHM applications, which requires the measurement of low frequencies (10^{-1} Hz) and low amplitudes (10^{-2} m·s^{-2}), is verified through extensive laboratory tests. Furthermore, the MEMS accelerometer board is employed during a shaking table test for measuring the earthquake-induced vibrations on a stone pinnacle of the Washington D.C. National Cathedral. Results show that ALE

This research was part of a Ph.D. program funded at Università della Calabria, Italy by European Union social fund (FSE - Fondo Sociale Europeo) within the POR Calabria FSE 2007 - 2013 project.

Alessandro Sabato, Domenico Luca Carní and Giancarlo Fortino are with Università della Calabria, 87036 Rende (CS), Italy. (e-mail: sabatoale@gmail.com; dlcarni@deis.unical.it; giancarlo.fortino@unical.it;).

Maria Q. Feng and Yoshio Fukuda are with Columbia University in the City of New York, NY 10025, USA. (e-mail: mqf2101@columbia.edu; yf2290@columbia.edu).

detects vibrations with a maximum error of nearly 2% when a comparison with Integral Electronics Piezoelectric (IEPE) accelerometers is performed.

This paper is organized as follows. After the section II, which describes ALE features, a detailed analysis of the carried out laboratory-based experiments is presented in section III, together with the results of the earthquake-induced vibration test on the stone pinnacle. A quantitative comparison of ALE with MEMS-based sensor state-of-the-art is presented in Section IV. Finally, conclusions are drawn and future work is briefly anticipated in Section V.

II. The Acceleration Evaluator Features

Usually, sensor boards include one or more sensing element(s), a computational core unit (microcontroller, ADC, flash memory, etc.), and a radio transmitter for wireless communication [17]. For the ALE design, a top-bottom approach has been employed [29]. Starting from an application instance (i.e. the necessity to monitor micro vibration with more accuracy than other MEMS-based sensor boards), the system platform has been developed using the most functional hardware to achieve this goal, and eventually by refining the circuits based on the run tests [30].

To reduce ALE complexity, power consumption, and to improve analyses accuracy, as many components as possible have been delocalized off-board. Thus, it is made of a transmitter and a receiver board. As shown in Figure 1, the custom-developed transmitter (powered by a 12 V rechargeable battery) consists of three sections.

The first one is the sensing element (i.e. accelerometer), which converts the acceleration quantity in voltage values. The second is the signal conditioning section, which supplies the excitation for the sensor, modulates in frequency the sensing element output, and adapts the signal for the next section. The latter is the Radio Frequency (RF) transmitter that modulates the signal conditioning section output and transmits it.

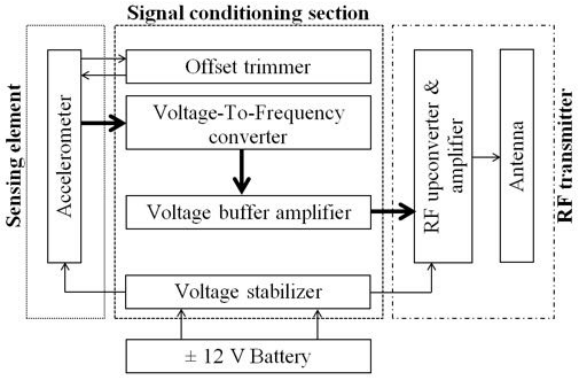

Fig. 1. Hardware diagram of ALE transmitter

The core components of the ALE sections are:

- a low floor-noise MEMS-based accelerometer SiFlex 1600SN.A MEMS-based accelerometer SF1600 [32], which can measure an acceleration range of ±29.42 $m \cdot s^{-2}$ with a resolution of $0.14 \cdot 10^{-3}$ $m \cdot s^{-2}$ for vibrations from 0 to 1500 Hz;
- a low power Voltage-to-Frequency (V/F) converter AD650, which transforms the analog signals measured by the sensor into frequency values minimizing the accuracy loss;
- a low power DC-to-DC converter (TMR3 1222E) used as voltage stabilizer for the ALE. It prevents from incorrect sensor readings and radio transmission problems as happened in other systems, which do not have a battery voltage up conversion and operate on unregulated battery voltage [11, 16, 27];
- a low power, 4 channels, 2.4 GHz Industrial Scientific and Medical (ISM) antenna used as temporary device for signal transmission to the receiver.

On the contrary of many other sensor boards (e.g. [11], [15], [23], [26]), only one sensing element, the SF1600 accelerometer, is embedded on the transmitter. As shown in Figure 1, unlike the conventional sensor boards, the V/F converter is employed instead of an ADC and on-board computational units miss. By using the V/F converter, it becomes possible to maximize the performance of the accelerometer. The resolution of a 12 V supplied ADC ($9.58 \cdot 10^{-2}$ $m \cdot s^{-2}$ at 10-bit, $2.39 \cdot 10^{-2}$ $m \cdot s^{-2}$ at 12-bit, and $1.50 \cdot 10^{-3}$ $m \cdot s^{-2}$ at 16-bit), would nullify the resolution of the SF1600. To optimize its resolution, the high-performance MEMS accelerometer selected in this study, should be matched with a 24-bit ADC ($5.84 \cdot 10^{-6}$ $m \cdot s^{-2}$), which is too power demanding for low-power wireless systems. Therefore, ALE converts the MEMS sensor output analog signals to Frequency Modulated (FM) signals using the V/F converter. The conversion speed is relatively slow compared with ADCs, but operating with converters having a sampling rate in the order of MHz and a narrow sensor bandwidth (0 - 1.5 kHz), it is possible to overcome this limitation [34]. Furthermore, to effectively measure micro vibrations, it is necessary overcoming the problem arising from the low signal-to-noise ratio output analog signals due to the electrical noise superimposed during the transmission. By converting the analog signal to a FM one, transmission becomes more stable and the robustness against the electrical noise is improved because of modulation characteristics [37].

Also unlike other sensor controller boards, ALE does not have any computational units on it. ALE demands the computational task to the receiver. It down-converts the RF signal in a baseband and demodulates the obtained FM signal. Then, the resulting analog signal is digitalized by a high-resolution Data AcQuisition board (DAQ) and post-processed using a Personal Computer (PC). By processing data with the external computer, it becomes possible to process larger amount of data and to perform more accurate analysis, which is one of the desirable feature in numerous engineering sectors. Moreover, by separating the microcontroller unit (MCU), which takes up a large share of the board's power consumption (between 15 and 25% [23], [33]), total power consumption can be dramatically reduced.

In Figure 2 the block scheme of the receiver is shown, which consists of three sections as well. The sections of the

receiver are similar to the transmitter sections with an opposite functionality.

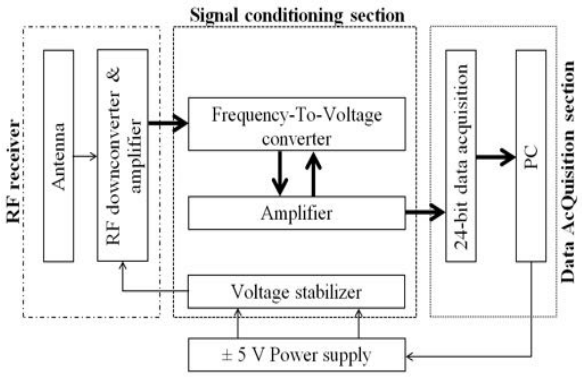

Fig. 2. Hardware diagram of ALE receiver

The first section is made of a RF receiver, which receives the transmitted signal and down-converts it in a Base-Band. Successively, the signal conditioning section reconstructs the original analog signal through the Frequency-to-Voltage (F/V) converter. Finally, the data acquisition section uses a 24-bit DAQ to digitalize the reconstructed signal and transfer this information to the PC. The DAQ has enough resolution for detection of micro vibrations. The PC manages the acquisition and analyses the acquired data by using a custom-developed Lab-View code.

The detailed description of the ALE transmitter and receiver board hardware can be found in [28].

III. The ALE Characterization Tests

To evaluate ALE performance, several laboratory tests were performed. In particular, the tests aim to: (i) demonstrate that ALE accuracy in measuring vibration relevant to SHM applications is comparable with the accuracy of traditionally used wired-based IEPE sensors and (ii) evaluate ALE consistency in measuring micro vibration for civil-engineering relevant applications. While the experiments performed for evaluating the hardware design consistency (i.e. calibration, evaluation of the maximum transmission distance, effect of battery charge), are not shown here for the sake of brevity but are reported in [28], the first set of tests is performed in a controlled environment. It refers to the case in which signals are stationary and the data recorded using ALE were statistically compared with those recorded using a IEPE accelerometer. On the other hand, the second set of test employed a traditional back-to-back comparison, both in time and frequency domains, with data recorded during a simulated earthquake.

A. ALE Characterization in the Case of Sinusoidal Vibration

In Figure 3 is shown the test bed for the evaluation of ALE performance in the case of a sinusoidal vibration. The test bed is made of an APS 113 shaking table, an IEPE accelerometer (PCB 39B04) as a reference sensor [38], and the ALE transmitter. Through this test, ALE sensitivity had been evaluated with low frequency and low amplitude vibration in a controlled environment. In the test, sinusoidal vibration with different frequencies (5, 2, 1, 0.5, and 0.2 Hz) and a Root Mean Square (RMS) value of nearly $1.60 \cdot 10^{-2}$ m·s^{-2} (1.63 mg) was used. Lower frequencies and amplitude were not available because of technical specifications of the shaking table. Both sensors were attached to the shaking table using threaded pin screws, according to the recommendations provided by ISO Standard [22]. For each frequency, a 5-minute measurement at 100 Hz sampling frequency was performed using the ALE receiver, placed 5 meter away from the transmitter, and the reference sensor.

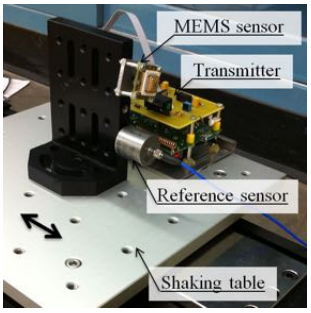

Fig. 3. Test bed for the ALE sinusoidal vibration characterization.

A statistical analysis was performed evaluating the measured value $\bar{x}$ and their dispersion standard deviation σ. The shaking table supplies a stationary sinusoidal vibration; therefore, each oscillation can be considered as one data set. For instance, when a sinusoidal signal having period of $T = 0.2$ s (5 Hz oscillation) and a record duration $L = 300$ s is considered, if the signal is divided in sub-signals each of them having duration $T = 0.2$ s, a total number of $L/T = 1500$ sub-signals (i.e. data set) are generated. Considering the 100 Hz sampling rate, each data set consists of 20 sample points. For each of these 20 points, it is possible to evaluate $\bar{x}$ and σ of the 1500 homologous data.

In Fig.4 is shown the trend of the reference sensor results mean value (continuous line) and the dispersion interval (dashed line) with distance $\pm \sigma$ from the mean value. Moreover, in the figure are reported the results obtained by using the ALE (diamond). This figure highlight as the results with the two method are compatible. In fact, the results with the ALE are always included in the dispersion interval of the reference sensor.

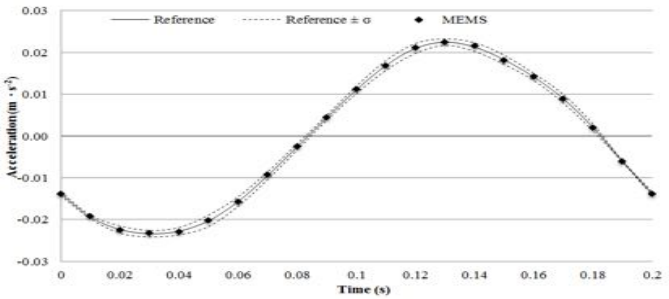

Fig. 4. Reference and MEMS sensors measured values and dispersion (5 Hz)

Figure 5 to 9 shows another data plots using same results in a recognizable way for the error comparison by using different acceleration frequencies. In these figures, the dispersion of the data points measured using ALE is normalized to the dispersion of the data points measured using the reference sensor (the data points are shifted using the

average values of the reference sensor as a baseline). In particular, the figures show: (i) the dispersion range in which reference sensor measured values are supposed to be (continuous line and vertical bars representing the reference sensor data dispersion, Reference ± σ), (ii) the MEMS sensor measured values evaluated as difference with the reference sensor measured values (diamond-shaped points represent the difference Reference - MEMS), (iii) the MEMS data dispersion range (dashed lines, MEMS ± σ).

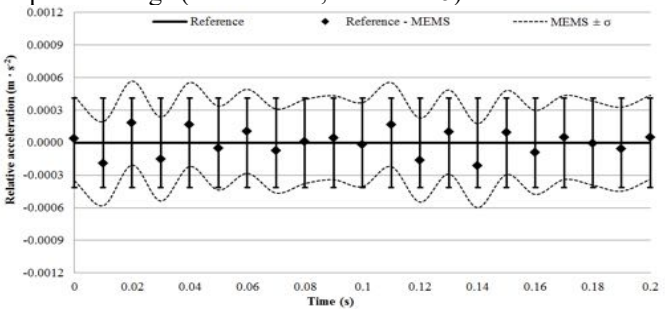

Fig. 5. Error comparison between measurement by ALE and measurement by the reference sensor (5 Hz)

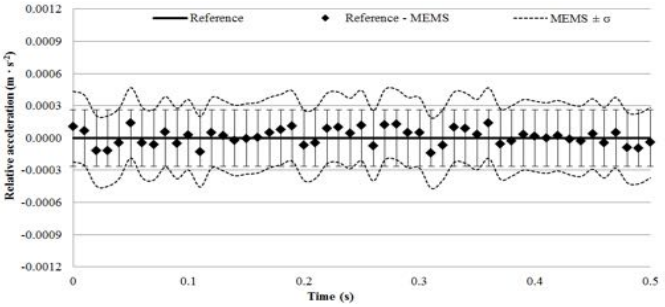

Fig. 6. Error comparison between measurement by ALE and measurement by the reference sensor (2 Hz)

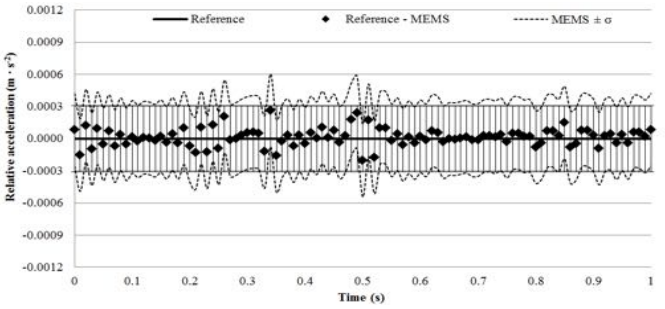

Fig. 7. Error comparison between measurement by ALE and measurement by the reference sensor (1 Hz)

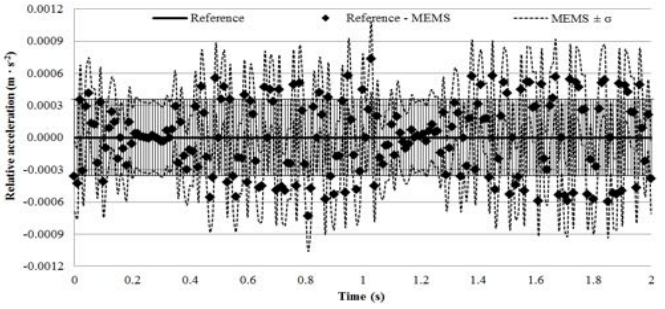

Fig. 8. Error comparison between measurement by ALE and measurement by the reference sensor (0.5 Hz)

The intersection between the two intervals (Reference ± σ and MEMS ± σ) highlights the compatibility of the results between the two sensors. By analyzing the plots, a substantial correspondence is observed in recorded data.

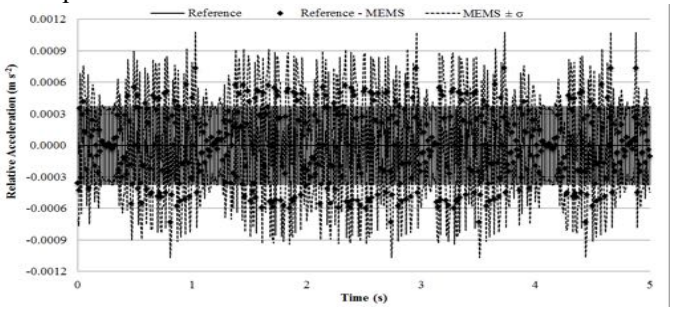

Fig. 9. Error comparison between measurement by ALE and measurement by the reference sensor (0.2 Hz)

The measurement values by ALE are constantly within the range of the dispersion measured by the reference sensor when frequency is higher than 0.5 Hz. For lower frequencies, several measurement values are out of the range. This result demonstrates that measurement errors increase as the frequency of the vibration decreases.

B. Measurement of Structural Seismic Response

Finally, to evaluate ALE efficacy in monitoring vibration of real engineering structures, a shaking table test on an actual structure model had been performed. In particular, ALE was used for evaluating the earthquake-induced vibrations on a special lab-scale model of a stone pinnacle, and its performance was compared with that of an IEPE accelerometer PCB 39B04 as a reference sensor. Figure 10 shows a 2,500 kg, 3 m high pinnacle model of the Washington D.C. National Cathedral, which is placed on an ANCO/MTS Hydraulic 2 Ton shaking table. As shown in the same figure, the ALE MEMS-based accelerometer and the reference sensor were placed on top of the pinnacle.

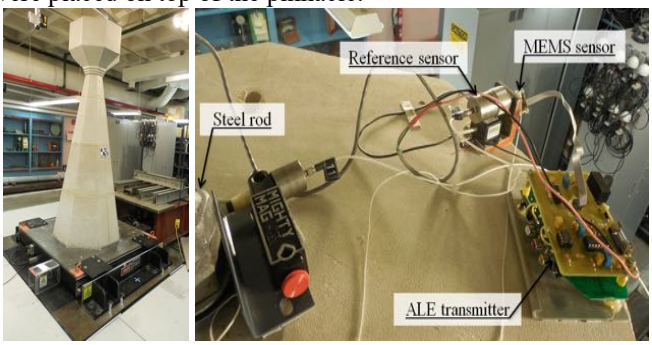

Fig. 10. Pinnacle model (left) and sensors installation (right)

The structure was subjected to a simulated uniaxial acceleration time history (TH) input, which is based on the actual seismic vibration recorded by the Corbin, VA seismograph station on August 23rd, 2011. The features of the simulated seismic vibration (50% of the original record) are listed in Table I.

TABLE I
EARTHQUAKE INPUT FEATURES

Duration (s)	PGA ($m \cdot s^{-2}$)	I_A ($m \cdot s^{-1}$)	f_1 (Hz)	f_2 (Hz)	f_3 (Hz)
23.00	1.56	0.21	0.76	1.03	1.61

In this table, the Peak Ground Acceleration (PGA), the earthquake's first-three fundamental frequencies f_i, and the Arias Intensity I_A (a measure of the strength of a ground motion of the seismic vibration) are shown [5].

During the test, the vibration was monitored with 100 Hz sampling frequency using an external DAQ system connected to the ALE receiver and the IEPE sensor. Results are plotted in Figures 11 and 12 where the THs recorded with the two sensors at two different times are reported and the excited frequencies, evaluated through a Fast Fourier Transform (FFT) analyses, are highlighted.

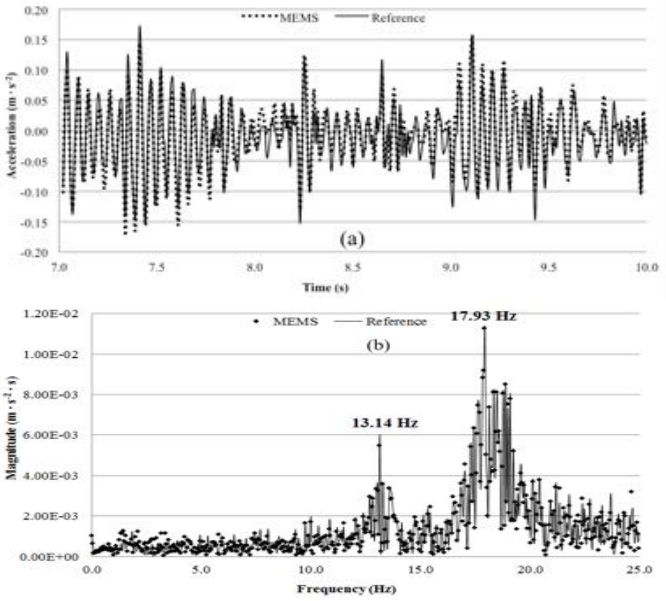

Fig. 11. Comparison of measurements by the two sensors in time domain (a), structural natural frequencies (b) (amplitude range: 10^{-2} - 10^{-1} m·s^{-2})

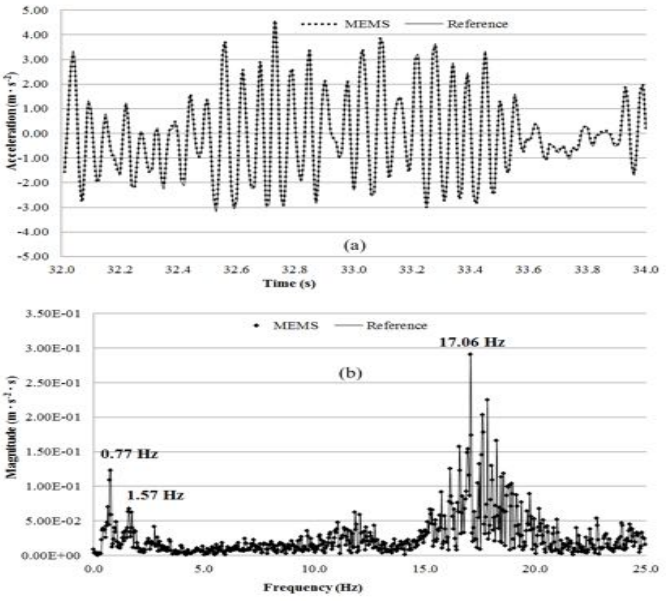

Fig. 12. Comparison of measurements by the two sensors in time domain (a), structural natural frequencies (b) (amplitude range: 10^{0} m·s^{-2}).

In particular, Figure 11 refers to vibrations produced by the shaking table supporting machineries (e.g. pump, oil circuit, etc.). They can be considered as ambient vibrations characterized by low-amplitude (10^{-2} - 10^{-1} m·s^{-2}) and used for evaluating the natural frequency of the pinnacle (13.14 Hz and 17.93 Hz). On the other hand, Figure 12 refers to the high-amplitude earthquake-induced seismic vibrations (amplitude range: 10^{0} m·s^{-2}) and it allows detecting the characteristic frequencies of both the earthquake (0.77 Hz, 1.03 Hz, and 1.57 Hz) and the pinnacle (17.06 Hz). As shown in the figures an excellent agreement between data recorded with the two sensors is observed. Table II lists a summary of the obtained results, where the I_A, the PGA, and the f_i recorded with the ALE and the reference sensor are numerically compared, and an evaluation of the committed relative error ε is carried out.

TABLE II
SUMMARY RESULTS FOR THE PINNACLE COMPARATIVE TEST

Quantity	MEMS	Reference	ε (%)
PGA ($m \cdot s^{-2}$)	4.518	4.517	0.02
I_A ($m \cdot s^{-1}$)	4.89	4.99	-2.08
f_1 (Hz)	0.77	0.77	
f_2 (Hz)	1.03	1.03	
f_3 (Hz)	1.57	1.57	
f_4 (Hz)	13.14	13.14	
f_5 (Hz)	17.06	17.06	

As show in the table, an excellent agreement between the measurement results of two sensors was observed. The PGA ant the I_A values are close to each other (relative errors equal to 0.02% and -2.08% respectively). This means that ALE can detect the peak acceleration acting on a system and the incident energy as well, with the same accuracy of a high sensitivity, wire-based, IEPE accelerometer. Furthermore, the frequency domain analyses show the same conclusions.

Since the recorded earthquake signal is non-stationary, a time-frequency analysis is performed on both datasets and results are plotted in Figure 13.

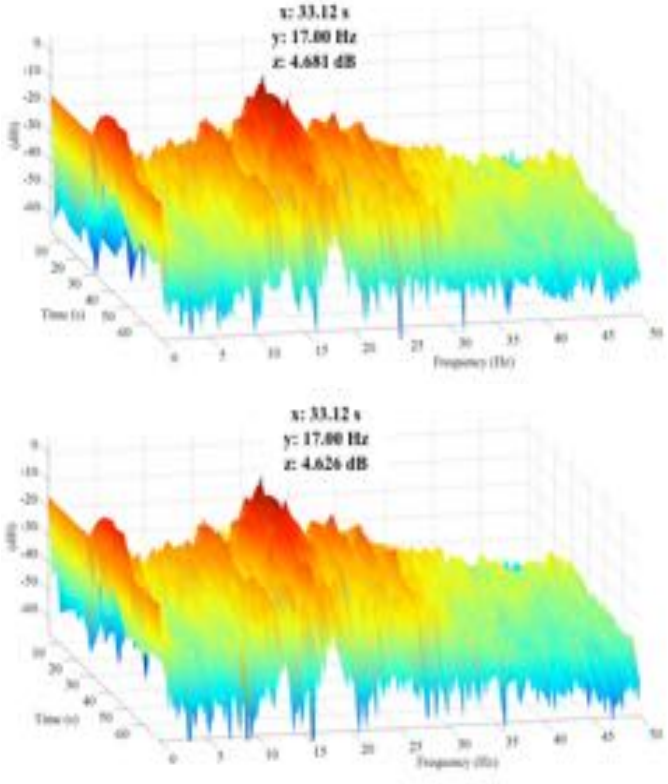

Fig. 13. Comparison of time-frequency analyses of the measurement by ALE

(top) and measurement by the reference sensor (down).

No significant differences can be observed in the two plots. In particular, when the central part of the earthquake is considered (t = 33.12 s), the two devices report the same value (17.00 Hz) as the fundamental frequency of the stone pinnacle. The error committed on the magnitude, equal to 1.18%, is consistent with the errors reported in the other tests. The small differences with frequency values listed in Table III are due to different integration methods used. Through this test, it is confirmed that ALE has an equal effectiveness to high performance sensors, those are usually employed for SHM, even for vibration around 1 Hz. Moreover, correspondence in the frequency domain was also confirmed in the earthquake characteristic frequencies (f_1, f_2, and f_3), as well as in the natural frequencies of the pinnacle (f_4 and f_5).

IV. Related Works

ALE has compared with several other academia-built prototypes and commercially available sensor boards for structural vibration detection [18], [19]. Among the most relevant ones, it is possible to find studies of Kurata el al. [15], Ruiz Sandoval et al. [26], Pakzad et al. [23], and Jo et al. [12], which are summarized in Table III and compared with the ALE features.

TABLE III
AVAILABLE SENSOR BOARDS SUMMARY AND COMPARISON WITH ALE

Study (-)	Sensing Range ($m \cdot s^{-2}$)	Bandwidth (Hz)	ADC (bit)	ADC Res. (10^{-3} $m \cdot s^{-2}$)	Board Res. (10^{-3} $m \cdot s^{-2}$)
Kurata [15]	±19.61	5 - 50	10	92.08	43.85
Ruiz-Sand. [26]	±19.61	2 - 400	10	23.94	1.24
Pakzad 1 [23]	±19.61	DC - 400	16	0.37	1.24
Pakzad 2 [23]	±0.98	0.20 - 25	16	0.37	0.31
Jo 1 [12]	±19.61	DC - 400	16	0.37	1.24
Jo 2 [12]	±1.96	1 - 15	16	0.37	0.43
ALE	±29.42	0.20 - 1500	-	-	0.19

As it is observed, in their research Kurata et al. used a commercially available sensor board embedding a low-cost, high noise-floor level sensor (i.e. ADXL202 [1]) and a 10-bit ADC, features not suited for SHM. The board only has the capability to detect high-amplitude vibrations. Ruiz-Sandoval et al. improved the same board by using a high-performance accelerometer (SD-1221L [31]), however, due to the 10-bit ADC the resolution is still limited to $23.94 \cdot 10^{-3}$ $m \cdot s^{-2}$. Also, the system can detect only above 2 Hz frequency vibrations. On the other hand, Pakzad et al. proposed a customized board using the same high-performance with a 16-bit ADC. In this case, the limiting factor to the measurement resolution became the installed sensor ($1.24 \cdot 10^{-3}$ $m \cdot s^{-2}$). For this reason, sensor bandwidth and measurement range were decreased from 400 Hz to 25 Hz and from ±19.61 $m \cdot s^{-2}$ to ±0.98 $m \cdot s^{-2}$ respectively to improve sensor's resolution and matching it to that of the embedded ADC ($0.37 \cdot 10^{-3}$ $m \cdot s^{-2}$). Analogously, Jo et al. in their study, artificially reduced the sensing range and the bandwidth for achieving a resolution of $0.43 \cdot 10^{-3}$ $m \cdot s^{-2}$ and a lower frequency limit of nearly 1 Hz using a customized design 16-bit ADC.

As listed in the table, ALE achieves superior performance without modification of the accelerometer features. In particular, maintaining a wide bandwidth (0.2 - 1500 Hz) and the full sensing range (±29.42 $m \cdot s^{-2}$), the best resolution and the lower detectable frequency are achieved compared with the presented systems. Furthermore, since no bandwidth reduction is applied, ALE can be used as multi-purpose device for monitoring systems, which have higher vibration frequencies as well.

V. Conclusions

In this study, ALE, a novel wireless MEMS accelerometer board embedded with a V/F converter, is proposed and developed for the purpose of SHM. This system, to improve the measurement resolution without modifying and limiting any of the embedded sensor features, employs a V/F converter, which creates the Frequency Modulated signals for high-accuracy measurement and low-noise wireless data transmission. Unlike most of the conventional MEMS-based wireless sensing systems, those have the bandwidth and resolution limitations, the developed system does not limit the performance of the embedded MEMS accelerometer. In addition, in order to reduce the power consumption and achieve accurate measurement, the computational section is delocalized off-board. In a series of laboratory tests, the ALE capability of measuring micro vibration (frequency up to 0.2 Hz and amplitude in the order of 10^{-2} $m \cdot s^{-2}$) was compared with IEPE sensors. Moreover, a shaking table test, using a 2,500 kg and 3 m high pinnacle model and the simulated earthquake-induced seismic vibration was conducted. As a result, the detected errors in frequency and time domains (2%) were small enough compared with the wire-based high-performance accelerometers, and ALE effectiveness for SHM applications was also confirmed.

Using ALE, it becomes possible to develop a monitoring system, which can accurately detect vibration phenomena without interfering, due to absence of cables, with the functions and architectural features of large-sized aging structures such as churches, monuments, and sculptures. Further developments of the prototype may consist of using the accelerometer board as a sensing node within Wireless Sensor Network [8] designing star-type topology first and more complex topologies later. The absence of on-board ADCs may reduce the conversion time-delay and may help if time-synchronizations have to be guaranteed in different nodes of the network.

References

[1] ADXL202/ADXL210: Low Cost ±2g/±10g dual axis iMEMS accelerometers with digital output, Available online: http://www.analog.com (accessed on Sep. 2014).

[2] J. Burrel, T. Brooke, and R Beckwith, "Vineyard computing: sensor networks in agricultural production," *IEEE Pervasive computing*, vol. *3,* no. *1,* pp. *38-45,* Jan, 2004.

[3] M. Calebi, "Seismic instrumentation of buildings (with emphasis on federal buildings)," US geological survey, Meno Park, CA,Abbrev. State, Rep. *0-7460-68170*, 2002.

[4] A. Camilli, C.E. Cugnasca, A.M. Saraiva, A.R Hirakawa, and P. Correa, "From wireless sensor to field mapping: anatomy of an application for precision agriculture," *Computers and electronics in agricolture*, vol. *58,* no. *1,* pp. *25-36,* Aug, 2007.

[5] A.K. Chopra, *Dynamics of Structures: Theory and Applications to Earthquake Engineering, 4th ed.* Prentice Hall, Boston, 2012.
[6] W. Dargie, "Dynamic power management in wireless sensor networks: state-of-the-art," *IEEE Sens. J.*, vol. *12, no.5,* pp. *1518-1528,* Apr, 2012.
[7] L. Dong, and K. Zhang, "Sensing and control of MEMS Accelerometers using Kalman filter," in *Proc. CCDC*, Taiyuan, China, 2012, pp. *3074-3079.*
[8] G. Fortino, A. Guerrieri, G. M. P. O'Hare, and A. G. Ruzzelli, "A flexible building management framework based on wireless sensor and actuator networks," *J. Network and Computer Applications*, vol. 35, no. 6, pp. 1934-1952, Jun, 2012.
[9] G. Fortino, R. Giannantonio, R. Gravina, P. Kuryloski, and R. Jafari: "*Enabling Effective Programming and flexible management of efficient body sensor network applications*". IEEE *T. Human-Machine Systems*, vol. 43, no.1, pp. 115-133, Jan, 2013.
[10] S. Gajjar, N. Choksi, M. Sarkar, and K. Dasgupta, "Comparative analysis of wireless sensor network motes," in *IEEE - SPIN*, Noida, India, 2014, pp. *426-431.*
[11] S.D. Glaser, "Some real-world application of wireless sensor nodes," in *Proc. SPIE*, San Diego, CA, 2004, pp. *344-355.*
[12] H. Jo, S. Sim, T. Nagayama, and B.F. Spencer, "Development and Application of High-Sensitivity Wireless Smart Sensors for Decentralized Stochastic Modal Identification," *J Eng. Mech.*, vol. *136, no.6,* pp. *683-694,* Jun, 2012.
[13] P. Juang, H. Oki, Y. Wang, M. Martonsi, L.S. Pehand and D. Rubenstein, "Energy-efficient computing for wildlife tracking: design tradeoffs and early experiences with ZebraNet," in *Proc. ASPLOS*, San Jose, CA, 2002, pp. *96-107.*
[14] S. Kim, S.N. Pakzad, D. Culler, J.W. Demmel, G.L. Fenves, S.D. Glaser, and M. Turon, "Health monitoring of civil infrastructures using wireless sensor networks," in *Proc. IEEE - ISPN*, Cambridge, MA, 2007, pp. *254-263.*
[15] N. Kurata, B.F. Spencer, and M. Ruiz-Sandoval, "Risk monitoring of buildings with wireless sensor networks," *Structural control and health monitoring*, vol. *12, no.3-4,* pp. *315-327,* Jun, 2005.
[16] M. Leopold, "Sensor Network Motes: Portability and Performance," Ph.D. dissertation, Dept. Computer Science, Københavns Universitet, Copenhagen, Denmark, 2008.
[17] J.P. Lynch, "Decentralization of wireless monitoring and control technologies for smart civil structures," Ph.D. dissertation, Dept. of Civil and Env. Eng., Stanford Univ., Stanford, CA, 2002.
[18] J.P. Lynch, and K.J. Loh, "A summary review of wireless sensors and sensor networks for structural health monitoring," *Shock and Vib. Dig.*, vol. *38, no.2,* pp. *91-130,* 2006.
[19] J.P. Lynch, "An overview of wireless structural health monitoring for civil structures," *Phil. Trans. Royal Society*, vol. *365, no.1851,* pp. *345-372,* Feb, 2007.
[20] A. Mainwaring, D. Culler, J. Polastre, R. Szewczyk, and J. Anderson, "Wireless sensor networks for habitat monitoring," in *Proc. ACM – WSNA*, Atlanta, GA, 2002, pp. *88-97.*
[21] M. Malinowsky, M. Moskwa, M. Felfmeier, M. Laibowitz, and A.J. Paradiso, "Cargonet: a low-cost micropower sensor node exploiting quasi-passive wakeup for adaptive asynchronous monitoring for exceptional events," in *Proc. SenSys*, Sydney, Australia, 2007, pp. *145-159.*
[22] Mechanical vibration and shock - Mechanical mounting of accelerometers, ISO 5348:2007, 2007.
[23] S. N. Pakzad, G.L. Fenves, S. Kim, and D. Culler, "Design and implementation of scalable wireless sensor network for structural monitoring," *J. Infrast. Sys.*, vol. *14, no.1,* pp. *89-101,* Mar, 2008.
[24] S. N. Pakzad, "Development and deployment of large scale wireless sensor network on a long-span bridge," *Smart Struct. and Sys.*, vol. *6, no.5-6,* pp. *525-543,* June, 2010.
[25] N. Raveendranathan, S. Galzarano, V. Loseu, R. Gravina, R. Giannantonio, M. Sgroi, R. Jafari, and G. Fortino, G., "From Modeling to Implementation of Virtual Sensors in Body Sensor Networks," *Sensors Journal, IEEE* , vol.12, no.3, pp. 583,593, Mar, 2012.
[26] M. Ruiz-Sandoval, B.F. Spencer, N. Kurata, "Development of a high sensitivity accelerometer for the Mica platform," in *Proc. IWSHM*, Stanford, CA, 2003, pp. *1027-1035.*
[27] Ad. Sabato, and Al. Sabato, "Construction and Validation of Small Electro-mechanical Vibration Sensors," *I. J. Comp. Met. and Expe. Meas.*, vol. *1, no.1,* pp. *72-79,* Jan, 2012.
[28] A. Sabato, and M.Q. Feng, "Feasibility of frequency-modulated wireless transmission for a multi-purpose MEMS-based accelerometer," *Sensors*, vol. *14, no.9,* pp. 16563-16585, Sep, 2014.
[29] A. Sangiovanni-Vincentelli, L. Carloni, F. De Bernardinis, F., and M. Sgroi, "Benefits and challenges for platform-based design," in *Proc. 41st annual Design Automation Conference*, pp. 409-414, June 2004.
[30] A. Sangiovanni-Vincentelli, and G. Martin, "Platform-based design and software design methodology for embedded systems," IEEE Design & Test of Computers, vol. *6*, pp. 23-33, June 2001.
[31] SD-1221: Low-noise Analog Accelerometer. Available online: http://www.silicondesigns.com/pdfs/1221.pdf (accessed on Sep. 2014).
[32] SF1600SN.A: Single axis best in class seismic accelerometer, Available online: http://www.colibrys.com (accessed on Apr. 2014).
[33] A. Sinha, and A. Chandrakasan, "Dynamic power management in wireless sensor networks," *IEEE Des. And Test of Comp.*, vol. *18, no.2,* pp. *62-74,* Aug, 2001.
[34] N.F. Thornhill, R. Zunino, and S. Rovetta, *Elettronica Analogica, 2th ed.* McGraw-Hill, Milan, 1999.
[35] T. Torfs, T. Sterken, S. Brebels, J. Santana, R. van den Hoven, V. Spiering, N. Bertsch, D. Trapani, and D. Zonta, "Low power wireless sensor network for building monitoring," *IEEE Sens. J.*, vol. *13, no.3,* pp. *909-915,* Jan, 2013.
[36] D.H Wang, and W.H. Liao, "Wireless transmission for health monitoring of large structures," *Inst. and Meas., IEEE Trans. on*, vol. *55, no.3,* pp. *972-981,* Jun, 2006.
[37] M.J. Whelan, M.V. Gangone, and K.D. Janoyan, "Highway bridge assessment using an adaptive real-time wireless sensor network," IEEE Sensors Journal, vol. 9, no. 11, pp. 1405-1413, Nov, 2009.
[38] 393B04: ICP Seismic Accelerometer. Available online: http://www.pcb.com/products.aspx ?m=393C (accessed on Apr. 2014).

Alessandro Sabato received the B.S. and the M.S. with full marks in environmental engineering and the Ph.D. degree in mechanical engineering from University of Calabria, Italy in 2006, 2010, and 2014, respectively.
He was with Columbia University at the Department of Civil Engineering and Engineering Mechanics (CEEM) from March 2013 to June 2014 as visiting Ph.D. student and staff-associate from February to June 2014.
His research and work interests include: environmental acoustics, noise and vibration control, wireless MEMS-based technologies, sensor-based structural health monitoring, energy from renewable sources, and HVAC systems. He is author of several publications in these fields.

Maria Q. Feng received the Ph.D. degree in mechanical engineering from the University of Tokyo, Japan, in 1992.
She has been Professor of Civil and Environmental Engineering at UC Irvine, from 1992 until 2011, with a joint appointment at the Department of Electrical Engineering and Computer Science. Since January 2012, she joined Columbia University as Renwick Professor at the Department of Civil Engineering and Engineering Mechanics (CEEM).
Her research interests are primarily in safety and security of civil infrastructure systems, focusing on innovative and interdisciplinary science and technology for sensors, health monitoring, and damage assessment. She has published near 350 journal and conference proceeding papers on these

subjects and she was the recipient of numerous awards and honors.

Yoshio Fukuda was born in Yamaguchi, Japan in 1976. He received the B.S. degree in product system engineering from Ube National College of Technology, Yamaguchi, Japan, in 1999 and the M.S. and Ph.D. degrees in mechanical engineering from Nagasaki University, Nagasaki, Japan, in 2001 and 2004 respectively.

He is currently an Associate Research Scientist with the Department of Civil Engineering and Engineering Mechanics (CEEM) at Columbia University, New York.

His research interests include visual sensing, man machine interface, human body sensing devices, and civil structure health monitoring.

Domenico Luca Carní achieved the master's degree in Computer Engineering from the University of Calabria in 2003. In 2006, he received the Ph.D. degree in Systems and Computer Engineering from the same university. At the moment, he is joining the Department of Informatics, Modeling, Electronics and Systems (DIMES), University of Calabria, as Assistant Professor of Electric and Electronic Measurements. His current research interests include the measurement on telecommunication systems, characterization of digital to analog and analog to digital converters, digital signal processing for monitoring and testing, virtual instrumentation and distributed measurement systems.

Giancarlo Fortino (SM'12) received the Laurea (B.S and M.S) and Ph.D. in computer engineering from the University of Calabria, Italy, in 1995 and 2000, respectively.

He is currently an Associate Professor of Computer Engineering (since 2006) with the Department of Informatics, Modeling, Electronics and Systems (DIMES), University of Calabria. He holds the scientific national Italian habilitation for Full Professor and he is also Guest Professor of Computer Engineering at the Wuhan University of Technology, China.

He authored over 230 publications in journals, conferences, and books. His research interests include distributed computing, wireless sensor networks, software agents, cloud computing, multimedia networks.